Journal of Applied Physics

Direct and inverse magnetoelectric effects in $HoAl_3(BO_3)_4$ single crystal

Cite as: J. Appl. Phys. **115**, 174103 (2014); https://doi.org/10.1063/1.4874270
Submitted: 30 December 2013 . Accepted: 20 April 2014 . Published Online: 02 May 2014

A. L. Freydman, A. D. Balaev, A. A. Dubrovskiy, E. V. Eremin, V. L. Temerov, and I. A. Gudim

AIP Publishing

Direct and inverse magnetoelectric effects in $HoAl_3(BO_3)_4$ single crystal

A. L. Freydman, A. D. Balaev, A. A. Dubrovskiy, E. V. Eremin, V. L. Temerov and I. A. Gudim
Kirensky Institute of Physics, Russian Academy of Sciences, Siberian Branch, Krasnoyarsk 660036, Russia

(Received 30 December 2013; accepted 20 April 2014; published online 2 May 2014)

The direct (ME_H-) and inverse (ME_E-) magnetoelectric effects in the $HoAl_3(BO_3)_4$ single crystal are studied. Temperature and magnetic field dependences of permittivity of the crystal are investigated. A relation between the investigated effects was established. It was found that the magnetoelectric effect can exist in crystals without magnetic order or spontaneous polarization. It was shown that the phenomena investigated are due to magnetostriction or magnetoelastic effect. The thermodynamic potential was considered for describing magnetoelectric effect at low magnetic fields. The results obtained are explained within a proposed qualitative microscopic model, based on interplay of configuration of 4f- electron subshell of the rare-earth element and applied magnetic or electric field. © *2014 AIP Publishing LLC*. [http://dx.doi.org/10.1063/1.4874270]

INTRODUCTION

Coexistence of the magnetic order and spontaneous electric polarization in multiferroic materials has been an object of study in condensed matter physics. The interest in these systems is due to a great number of fundamental effects exhibited by multiferroics[1–5] with a multitude of possible applications.[6–8] According to the definition given in study by Eerenstein *et al.*,[9] multiferroics are a class of compounds with any two or all three of the following ordering types: spontaneous magnetic moment, spontaneous dipole moment, and spontaneous deformation.

However, the ferroelectric phase rarely coexists with the magnetic order and even when it does, they interact very weakly.[10] There are two types of multiferroics: in the multiferroics of the first type, the magnetic and ferroelectric phase transitions do not depend on one another; in the multiferroics of the second-type, the phase transitions occur simultaneously and are interrelated. In the latter case, the interaction between the magnetic and ferroelectric subsystems can be very strong.[3,11,12]

It is still unclear which mechanism is responsible for the magnetoelectric effect at the microscopic level. Following the experimental observation of the linear magnetoelectric interaction,[13] a number of works devoted to the search for and investigation of materials revealing this effect were published.[14–16] The materials revealing the magnetoelectric effect exhibit the dependence of polarization on an applied magnetic field, i.e., the ME_H-effect, or the magnetization variation in an applied electric field, i.e., the ME_E-effect. Study of the magnetic symmetry and thermodynamic potential of an investigated system usually yields some information on the magnetoelectric effect. In particular, the presence of the center of the spatiotemporal inversion symmetry suggests the magnetoelectric effect, which is expressed by the EH term in the thermodynamic potential, while the presence of the spatial inversion symmetry only suggests the bilinear magnetoelectric effect, the corresponding terms of which in the thermodynamic potential are EEH or EHH.[2,17]

The EH and EHH effects are measured by dynamic and quasi-steady-state methods. The quasi-steady-state method for measuring the ME_H-effect[18,19] is a direct technique applicable up to very strong static magnetic fields. This method is sufficiently accurate, since it allows measuring a magnetic-field-induced charge directly without calibration. The technique for measuring the ME_E-effect developed by Astrov *et al.*[20] allows the magnetization to be measured in an applied electric field.

Among substances revealing the magnetoelectric effect is the borate family $RM_3(BO_3)_4$, where R is a rare-earth ion or Y and M is an Al, Fe, Ga, Sc, or Cr ion. Crystals in this family have the R32 space group,[21] which determines the absence of the inversion center. The MO_6 octahedra sublattice forms a helical chain along the *c* axis with the exchange interaction of 3d elements; the rare-earth ions form RO_6 prisms and are isolated from one another by BO_3 triangles, i.e., there is no the R–O–R interaction.[22] Both the BO_3 triangles and RO_6 prisms are coupled with three MO_6 chains.

In study by Liang *et al.*,[23] the authors reported the giant ME_H magnetoelectric effect in the $HoAl_3(BO_3)_4$ crystal. It is noteworthy that this material is not a multiferroic in the ordinary sense, since it is not magnetically ordered.[23–25] As was shown in study by Chaudhury *et al.*,[26] the transition element, e.g., iron, is not necessary for the existence of the magnetoelectric effect. It has been recently demonstrated that the value of magnetoelectric polarization in $HoFe_3(BO_3)_4$ and $HoAl_3(BO_3)_4$ is mainly caused by the value of magnetostriction in these compounds.[27] However, the processes occurring at the microscopic level are still not fully understood. The magnetoelectric interaction, and in particular, the role of a rare-earth ion, needs further investigation.

The aim of this study was to investigate the ME_E-effect and permittivity in the $HoAl_3(BO_3)_4$ crystal in order to clarify the microscopic mechanism responsible for this effect.

EXPERIMENTAL

Holmium aluminum borate $HoAl_3(BO_3)_4$ single crystals were grown from the flux. As in study by Liang *et al.*,[23] we use the orthogonal system of coordinates *(x, y, z)* with the *x* and *z* axes coinciding with the *a* and *c* crystallographic directions, respectively, and the *y* axis perpendicular to the *xz* plane. Samples under investigation were rectangular plates

cut parallel to the natural face $(11\bar{2}1)$ so that the x and z directions were in the plate plane and the y direction was perpendicular to it.

For the measurements of permittivity and the ME_H- and ME_E-effects, the sample faces were covered with a conductive epoxy adhesive. The ME_H-effect was studied by measuring a charge between two contacts on the opposite sides of the parallel-sided plate with a Keithley 6517B electrometer. Temperature and magnetic field were controlled with the use of a Physical Property Measurement System PPMS-9 (Quantum Design). Permittivity was investigated by the capacity measurements on an Agilent E4980A Precision LCR Meter. The ME_E-effect was measured by technique proposed by Astrov *et al*.[20] on an original setup.[28]

The magnetic properties of the grown crystals were investigated on a vibrating-coil magnetometer (Quantum Design) at temperatures of 3−300 K in magnetic fields up to 9 T.

A setup for measuring the ME_E-effect based on a vibrating-coil magnetometer is illustrated in Fig. 1. Sample 1 with plates 2 was placed in the center of pick-up coil 3 and an AC voltage with the frequency of 1 kHz from generator 4 was applied to the sample plates. As a result of the magnetoelectric effect, the magnetic moment of the sample changes periodically and an AC voltage is induced in pick-up coil 3 and detected by detector 5. Using this circuit, one can detect the magnetic moment variation along the axis of coil 3 only.

If the magnetic and electric subsystems of the crystal are coupled by the elastic interaction (piezoelectricity, piezomagnetism, magnetostriction, or electrostriction), it is reasonable to detect the signal at several harmonics, since the frequency of the crystal strain caused by the piezoelectric effect coincides with the AC voltage frequency (first harmonic). However, electrostriction is the quadratic function of the electric field strength E; therefore, the strain frequency exceeds the applied AC voltage frequency by the factor of 2 (second harmonic). The strain affects the magnetization of the sample via the magnetoelastic effect. Thus, the advantage of our measurement technique over the measurements of the ME_H-effect is that while measuring the first and second harmonic signals separately, we can determine the contributions of the piezoelectric effect (first harmonic) and electrostriction (second harmonic), whereas the ME_H-effect measurements cannot detect the electrostriction contribution, since the induced strain does not lead to the sample polarization variation due to electrostriction. As was mentioned by Schmid,[17] the drawback of the technique proposed by Astrov *et al*.[20] is the necessity of the calibration of the entire measuring circuit. Synchronous detector 5 measures voltage U induced in pick-up coil 3 via magnetic moment variation ΔM of the sample and not the value of ΔM in itself. To compare the values of U and ΔM, the setup was calibrated.

External field H is induced by superconducting solenoid 6. Since magnetic field H is static, it does not contribute to the voltage induced in pick-up coil 3.

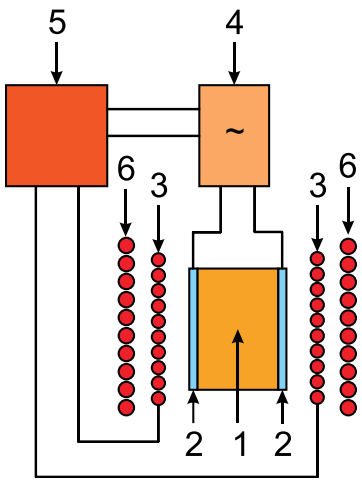

FIG. 1. Schematic circuit of the ME_E-effect measurements.

MAGNETIC MEASUREMENTS

Figures 2(a)–2(c) present the measured magnetization of the $HoAl_3(BO_3)_4$ sample vs applied magnetic field and temperature at different field directions. The shape of the presented dependences indicates that the crystal is paramagnetic and exhibits anisotropy of the magnetic properties. It can be seen in Fig. 2(a) that the magnetization grows in field H_z faster than in field H_x, although the maximum signal in the field $H \sim 90$ kOe is larger when the field is applied along the x axis. Figure 2(b) shows temperature dependences of the magnetization measured in different magnetic fields. Here, one can also see the anisotropy of the magnetic properties. Figure 2(c) shows the temperature dependence of the difference between magnetizations M_z and M_x measured in fields H_z and H_x, respectively.

It can be seen in Fig. 2(c) that the temperature dependence of the magnetization difference M_z-M_x is non-monotonic and the position of its maximum depends on the applied magnetic field. As the field is increased, the maximum shifts toward higher temperatures and its magnitude decreases. At the same time, in the field $H = 1$ kOe, the function $M_z-M_x(T)$ is relatively small and has no maximum. In the investigated compound, only Ho^{3+} ions have the magnetic moment; consequently, the anisotropy of the magnetic properties is explained by the fact that the magnetic moments of Ho^{3+} ions react differently to the magnetic field applied in different directions. In field H_z, the magnetic moments of Ho^{3+} ions align faster than in field H_x.

ME_H- AND ME_E-EFFECTS

According to the measurement results, the ME_E-effect $\Delta M(E, H, T)$ is a linear function of electric field E, but the slope of the function $\Delta M(E)$ strongly depends on magnetic field H. In Figure 3, the ME_E-effect is plotted in coordinates E and H; black and grey dots show the experiment and linear approximation, respectively. In our designation ΔM_{ij}, i is the direction along which the value of ΔM was measured and j is the direction of field E.

It can be seen in Fig. 3 that the linear approximation of the function $\Delta M(E)$ fits well the experimental data for both transverse (ΔM_{yx}) and longitudinal (ΔM_{yy}) effects. However, the ME_H-effect in this compound is nonlinear.[23]

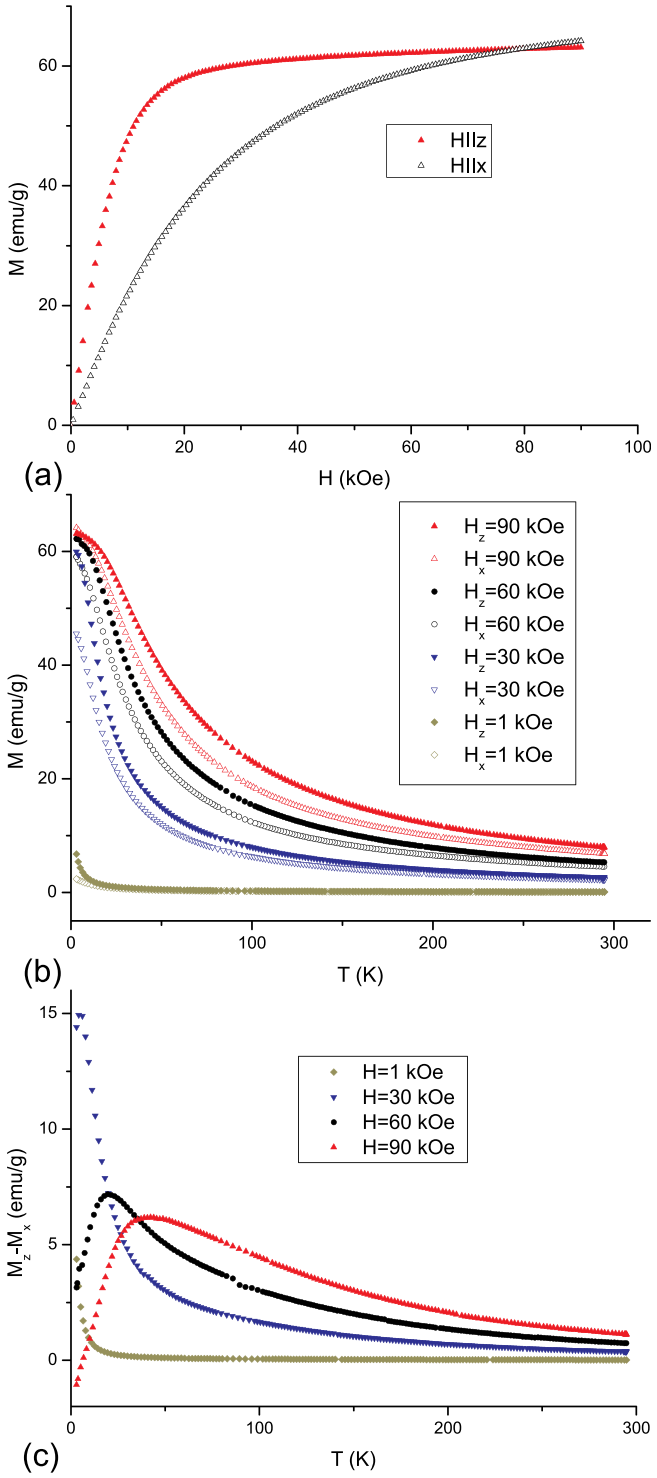

FIG. 2. (a) Field dependence of magnetization M(H) for the $HoAl_3(BO_3)_4$ crystal at different directions of a magnetic field and a temperature of 3 K. (b) Temperature dependence of magnetization M(T). (c) Temperature dependence of the magnetization difference $M_z - M_x$.

In addition, the linear magnetoelectric effect is possible only in magnetically ordered crystals, whereas, as mentioned above, $HoAl_3(BO_3)_4$ is paramagnetic, i.e., magnetically disordered. Nevertheless, the nonlinear effects can be met in magnetically disordered crystals.[29] This contradiction could be explained by consideration of higher harmonics, but we managed to detect the signal only at the first harmonic.

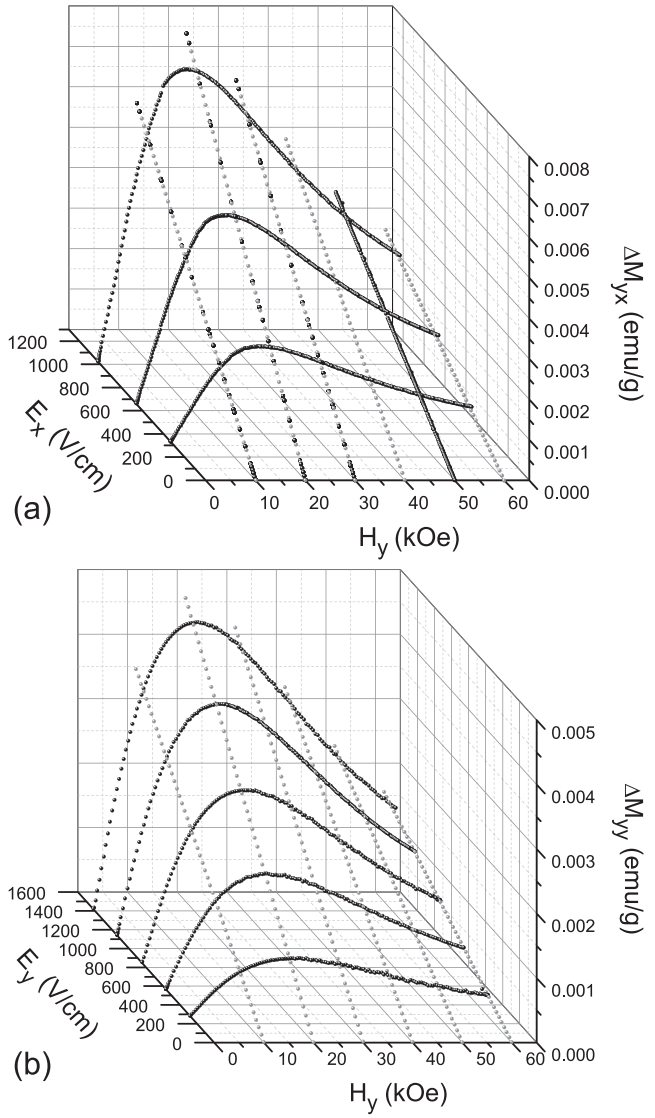

FIG. 3. Transverse (a) and longitudinal (b) ME_E-effect measured at the temperature T = 4.2 K.

Thus, in the thermodynamic potential there is no term αEH, but there are terms that yield the linear dependence of magnetization on field E and the nonlinear dependence on field H.

Figure 4 shows temperature and field dependences of the magnetoelectric susceptibility of the ME_E-effect $\beta_{ij} = \Delta M_{ij}/E_j$ for two measurement configurations; black and grey points correspond to the experiment and the approximation. In Figure 4(a), the electric field is applied along the *x* axis (transverse effect) and in Fig. 4(b), along the *y* axis (longitudinal effect).

One can see from the Figure 4 the maxima in the dependences $\beta_{yx}(H_y, T)$ and $\beta_{xx}(H_y, T)$ in fields H_y of 17.5 and 20 kOe at a temperature of 4.2 K for the transverse and longitudinal effects, respectively. Magnetoelectric susceptibility β_{yx} exceeds β_{yy} by a factor of 2. The ME_E-effect maximum shifts toward stronger magnetic fields as the temperature is increased, because thermal fluctuations prevent alignment of the magnetic moments along the applied magnetic field. In addition, thermal fluctuations explain a decrease in the ME_E-effect amplitude with increasing temperature.

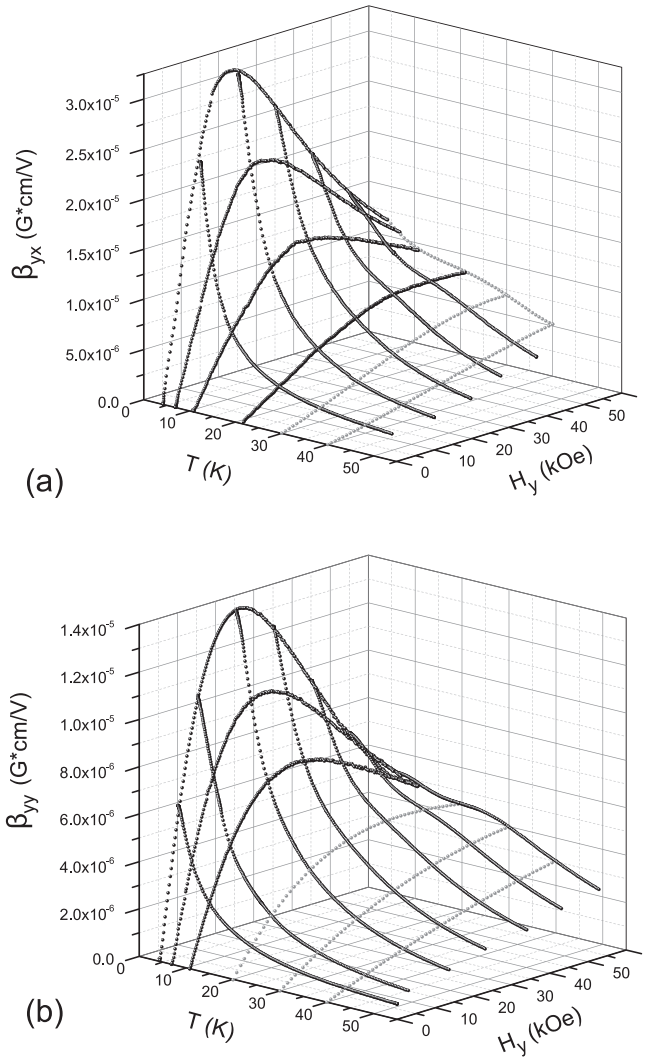

FIG. 4. Magnetoelectric susceptibility for transverse $\beta_{yx}(H_y, T)$ (a) and longitudinal (b) $\beta_{yy}(H_y, T)$ effect.

Figure 5 presents temperature and field dependences of magnetoelectric polarization ΔP_{yy} of the ME_H-effect. Magnetic field H was applied along the *y* axis; polarization was measured also along this axis.

The temperature dependencies show the growth of the effect with decreasing temperature. The field dependencies measured at different temperatures are qualitatively consistent with the analogous curves in study by Begunov *et al.*[24] It is important that the absolute value of the effect in our samples is smaller than that in the crystals investigated previously by a factor of 4. We attribute this difference to possible structural inversion twinning in our samples. It is well-known that in the crystal structure of trigonal rare-earth oxiborates with the huntite structure, the oxygen octahedra, in which Fe^{3+} (Al^{3+}, Ga^{3+}, or Sc^{3+}) ions are located, form a spiral chain along the three-fold axis. Depending on the crystal, the spiral can be both right- and left-hand twisted or mixed (twinning or chirality). The presence of twinning apparently leads to the situation when isomers with the right- and left-hand spirals make contributions of the opposite signs to the magnetoelectric polarization. When the magnetic field is applied, the charge is partially compensated, which

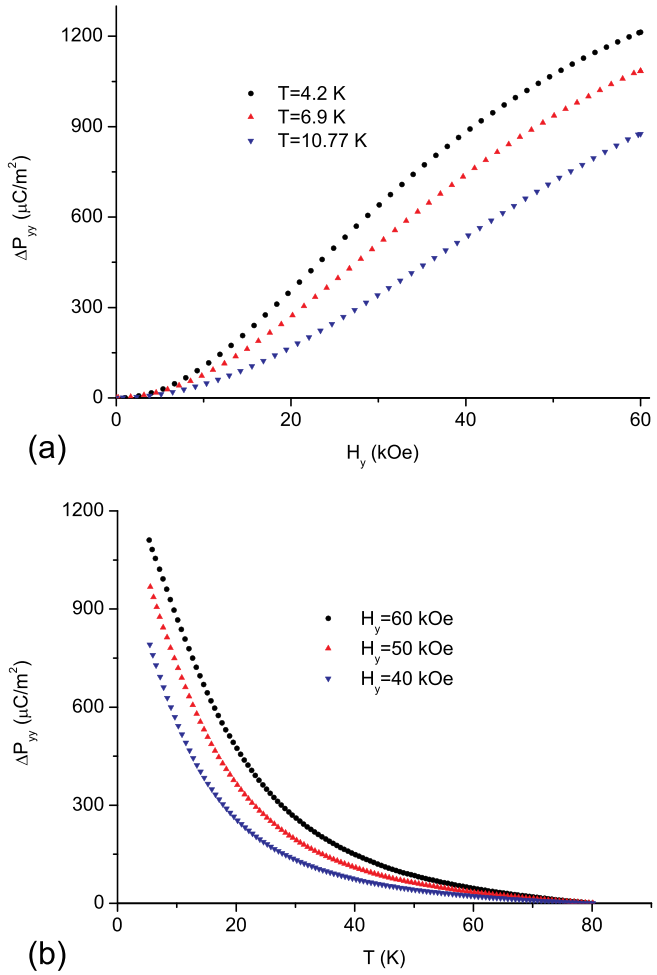

FIG. 5. Field (a) and temperature (b) dependences of the ME_H-effect ΔP_{yy}.

should eventually lead to a decrease in the absolute value of the effect.

In addition, we found that the shape of the dependence $\beta_{yy}(H)$ is similar to the shape of the ME_H-effect susceptibility function $\alpha_{yy}(H) = d(\Delta P(H))/dH$. The dependences $\alpha_{yy}(H)$ and $\beta_{yy}(H)$ are shown in Fig. 6 by the dotted and solid lines, respectively. It can be seen that the curves are the most

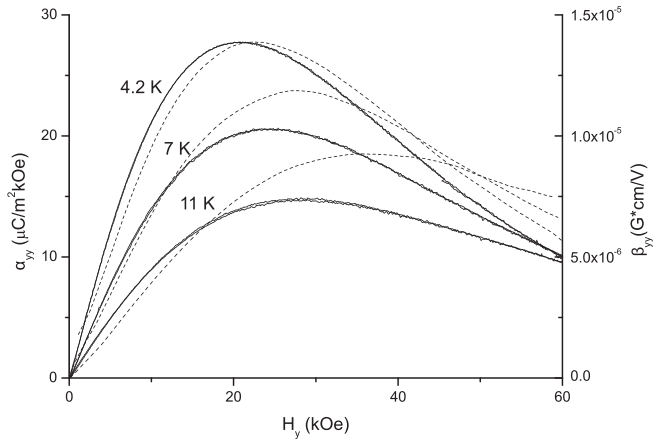

FIG. 6. Field dependences of magnetoelectric susceptibilities $\alpha_{yy}(H)$ (dotted line) and $\beta_{yy}(H)$ (solid line) at different temperatures.

similar in the low-temperature region, while, as the temperature increases, the maximum of α(H) shifts toward stronger magnetic fields more than the maximum of β(H).

PERMITTIVITY

Figure 7 shows the experimental temperature and magnetic field dependences of permittivity. The magnetic field was applied in the *y* direction of the crystal. Capacitance was measured along the *x* and *y* axes (Figs. 7(a) and 7(b), respectively). One can clearly see the anisotropy of the dielectric properties of the crystal. The permittivity measured in the *x* direction of the crystal, i.e., perpendicular to the magnetic field (Fig. 7(a)), decreases with increasing temperature and grows with increasing H_y, while the permittivity measured in the *y* direction of the crystal, i.e., parallel to the applied magnetic field (Fig. 7(b)), decreases with increasing temperature and magnetic field H_y.

It can be seen that at a temperature of 4.2 K, the value of ε_x grows by 7% and the value of ε_y decreases by 5.5% as magnetic field H_y increases to 60 kOe. The dependence ε_y(T) in strong fields H_y has the maximum at 20.5 K in a field of 50 kOe, which shifts toward higher temperatures as the field is increased.

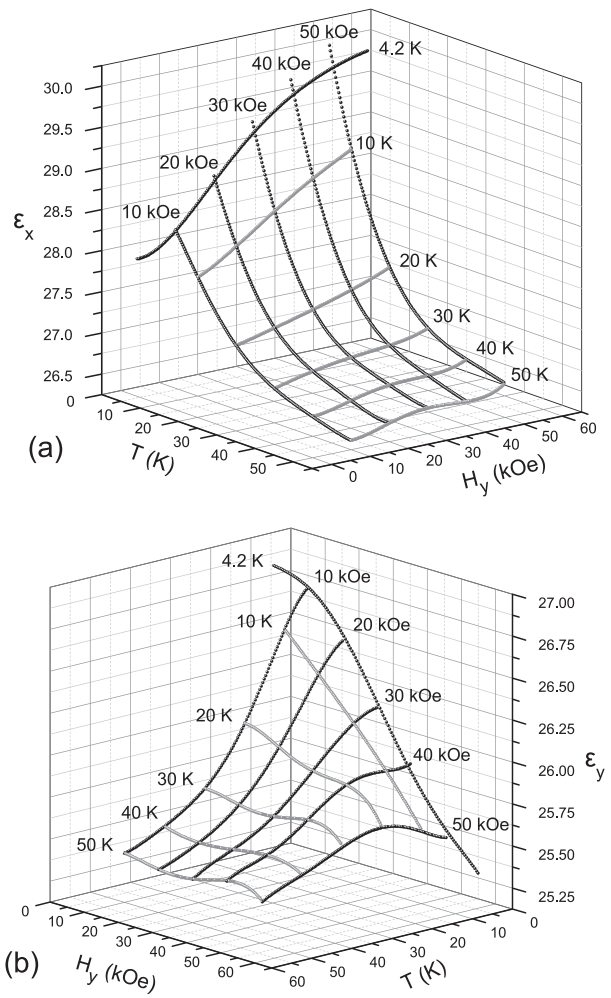

FIG. 7. Dependences ε_x(H_y, T) (a) and ε_y(H_y, T) (b) at f = 2 kHz.

THE THERMODYNAMIC POTENTIAL

For description of the magnetoelectric effect in $HoAl_3(BO_3)_4$ crystal at weak magnetic fields we can use the equation for the function of free enthalpy[18]

$$F(\mathbf{E},\mathbf{H}) = F_0 - P_i^s E_i - M_i^s H_i - \frac{1}{2}\varepsilon_0\varepsilon_{ij}E_iE_j - \frac{1}{2}\mu_0\mu_{ij}H_iH_j - \alpha_{ij}E_iH_j - \frac{1}{2}\beta_{ijk}E_iH_jH_k - \frac{1}{2}\gamma_{ijk}H_iE_jE_k\ldots \quad (1)$$

In (1) the component as $P_i^sE_i$ can be accepted only in pyroelectric, the contribution of spontaneous magnetization $M_i^sH_i$ can be accepted only in crystals with magnetic ordering; in our case of paramagnetic state of $HoAl_3(BO_3)_4$, these components vanish. The components $\frac{1}{2}\varepsilon_0\varepsilon_{ij}E_iE_j$ and $\frac{1}{2}\mu_0\mu_{ij}H_iH_j$ can be accepted for all symmetry groups. The contribution of the linear magnetoelectric effect $\alpha_{ij}E_iH_j$ is allowed only in some of the crystals with magnetic ordering, consequently in our case this component also vanishes,[30,31] as does the component of bilinear magnetoelectric effect $\frac{1}{2}\gamma_{ijk}H_iE_jE_k$, which is allowed only in groups with piezomagnetic effect. The component $\frac{1}{2}\beta_{ijk}E_iH_jH_k$ can be accepted in $HoAl_3(BO_3)_4$ crystal, because the crystal group R32 allows piezoelectricity.[32] Consequently, the thermodynamic potential for the $HoAl_3(BO_3)_4$ crystal will become

$$F(\mathbf{E},\mathbf{H}) = F_0 - \frac{1}{2}\varepsilon_0\varepsilon_{ij}E_iE_j - \frac{1}{2}\mu_0\mu_{ij}H_iH_j - \frac{1}{2}\beta_{ijk}E_iH_jH_k\ldots \quad (2)$$

After differentiating of Eq. (2) on H_i, we will find the expression for magnetization

$$M_k(\mathbf{E},\mathbf{H}) = \mu_0\mu_{ik}H_i + \beta_{ijk}E_iH_j\ldots \quad (3)$$

In Eq. (3), the first component is equal to the usual magnetization of the crystal in applied magnetic field. During the measurement of the ME_E-effect we are fixing only variable subcomponent of magnetization, which oscillates with the frequency of applied electric field (~1 kHz). Applied magnetic field H_j is permanent, so this component is not contributed in the results obtained. The component $\beta_{ijk}E_iH_j$ vanishes when $E_i = 0$ or $H_j = 0$; this fact is in good agreement with experiment (Fig. 3). Moreover, the function ΔM(H) in magnetic fields up to 5 kOe is linear (Figs. 3(a) and 3(b)). But in increasing magnetic fields, the function ΔM(H) becomes nonlinear. This fact points out on the necessity of considering components of the higher order for the full description of the ΔM(H,E) dependence.

After differentiating Eq. (2) on E_i, we will find the formula for the polarization

$$P_k(\boldsymbol{E},\boldsymbol{H}) = \varepsilon_0\varepsilon_{ij}E_j + \beta_{ijk}H_jH_k\ldots \quad (4)$$

During the measurements of the ME_H-effect the $E_j = 0$, so the first component does not contribute to the results of the experiment. In the work by Liang *et al.*,[23] at low magnetic fields (lower than 10 kOe), the ΔP(H) dependence has the square-law shape, which is in good agreement with

formula (4), but for a fuller description of ΔP(H) dependence it is necessary to consider of the components of higher order.

MICROSCOPIC MODEL

As is well-known, the orbital momentum of 4f transition elements is not frozen by the crystal field in contrast to that of 3d elements, as the ligand field is screened with the outer 5s and 5p orbitals. In former elements, the energy of the spin-orbit interaction is higher than the energy of the interaction between the crystal field and the orbit; as a result, both the spin and orbital magnetic moments participate in the formation of the magnetic properties. During magnetization of the crystal, the total magnetic moment J of an ion rotates, and the orientation of the entire 4f subshell changes.

When the orbital momentum is nonzero, the electron density distribution in the 4f subshell is non-spherical and, for a Ho^{3+} ion, the electron density can be presented as an ellipsoid of revolution flattened along the quantization axis.[33,34] This determines the uniaxial anisotropy of the magnetic properties of the $HoAl_3(BO_3)_4$ crystal. According to the magnetic measurement data (Fig. 2), the three-fold axis C_3 is the easy magnetization axis, i.e., the magnetic moments of Ho^{3+} ions are mainly parallel to the C_3 axis.

All the holmium ions in the crystal hold equivalent positions and are surrounded by a slightly twisted oxygen prism with a triangular base. Figure 8(a) shows the schematic of the electron density of the 4f subshell of a Ho^{3+} ion in the form of a flattened ellipsoid of revolution with its nearest oxygen surrounding. Without an external magnetic field, the 4f subshell of a holmium ion takes the position corresponding to the minimum overlap with oxygen ion shells (Fig. 8(a)). It can be seen that in this case the magnetic moment is directed along the *z* axis. It should be noted that in the demagnetized state, the magnetic moments of Ho^{3+} ions are distributed over the $+z$ and $-z$ directions; Figs. 8(a)–8(f) show only a half of ions with the magnetic moments codirectional with $-z$.

When external magnetic field H_z is applied, the magnetic moments of one half of the ions rotate by 180°. During the rotation of the magnetic moments, the striction caused by the 4f subshell orientation variation arises in the crystal. It can be seen in the figure that the electron shells of holmium and oxygen ions overlap stronger in rotation phase *b* than in phase *a*. Thus, additional electrostatic forces appear that cause the strain of the crystal lattice, reaching their maximum in phase *c* when the magnetic moment of a holmium ion lies in the *xy* plane. Figure 8(d) shows the projection of this phase onto the *xy* plane. It can be seen that the electrostatic forces acting on a holmium ion forming the side of oxygen ions numbered 12, 22, 13, and 23 differ from the forces acting from the side of ions 11 and 21, which leads to the shift of a Ho^{3+} ion in the *x* direction. Such a position of the 4f subshell can lead to a decrease in the twist angle of the oxygen prism, since oxygen ions 12 and 23 undergo a stronger effect of a holmium ion than ions 22 and 13. Thus, the occurrence of the electric dipole moment in this compound in an applied magnetic field, i.e., the ME_H-effect, can be caused by the shift of a holmium ion relative to the prism and the change in its twist angle.

As was shown by Liang *et al.*,[23] at the liquid helium temperature in a magnetic field applied along the *z* axis, the crystal undergoes positive magnetostriction λ_x, which reaches its maximum in a field of about 30 kOe. With a further increase in the field, λ_x drops to zero at about 55 kOe and then becomes negative and does not saturate at 70 kOe.

Such a complex behavior of magnetostriction, with a maximum present, can be explained within the qualitative model described above. With the magnetization up to phase *c*, the crystal expands due to the shift of oxygen ions; however, at the further rotation of the 4f subshell, crystal strain λ_x decreases, since in the terms of the electrostatic interaction, phases *b* and *e* are identical. This process occurs up to phase *e*, but, as was shown by Liang *et al.*,[23] after passing through zero, $\lambda_x(H)$ becomes negative and continues to decrease as the field is increased. This can be explained by assuming that the magnetic moments in the demagnetized state are not aligned strictly in the *z* direction as in Fig. 8(a), but are statistically distributed along this direction with some deviations that become smaller with increasing field. Consequently, the overlap of the electron shells also decreases, and as a result, the crystal compresses along the *z* axis.

The ME_E-effect can also be explained within the proposed model. An AC electric field applied to the crystal leads to the oscillating strains due to the inverse piezoelectric effect; i.e., the alternating strain of the crystal lattice occurs. As a consequence, the overlap of the electron shells of holmium and oxygen ions changes and a holmium ion, depending on the sign of the oxygen prism strain (extension or compression), appears either in a freer or a more constrained state. If this crystal is in external magnetic field H, then the 4f subshell of a Ho^{3+} ion will rotate under the action of the field and, due to the alternating strain of the oxygen surrounding, the angle between the direction of field H and the magnetic moment of an ion will oscillate relative to a constant value. In other words, in external electric field E, the

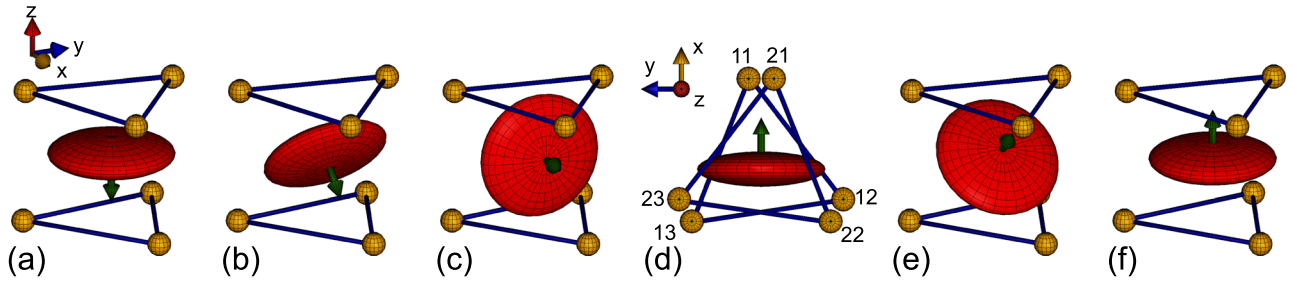

FIG. 8. Phases of rotation of Ho^{3+} ion at crystal magnetization (H||z).

magnetic susceptibility of the crystal changes due to the ligand field variation. Thus, in external magnetic field H, the angle between the direction of H and the magnetic moment of an ion oscillates. Now, it is clear that in the field $H = 0$ there should be no ME_E-effect, since the magnetic moments of holmium ions are statistically distributed over the $+z$ and $-z$ directions. Therefore, the crystal lattice strain can lead to the change in the orientation of the electron shells, but with the resulting magnetic moment remaining invariable. In strong magnetic fields H_x, the orientation of the 4f subshell corresponds to Figs. 8(c) and 8(d), where one can see that in this state the ME_E-effect should also be absent, since the oxygen prism strain can only shift a holmium ion in the direction of the field, but not rotate the magnetic moment. Thus, in the intermediate state (Fig. 8(b)), the magnetic susceptibility of the crystal appears the most sensitive to an AC electric field.

Our measurements of the ME_E-effect correspond to the case when an external magnetic field is applied in the y direction (Fig. 9). In this case, in strong magnetic fields the orientation of the 4f subshell relative to the oxygen surrounding differs from the case of H_x, as can be seen in Figs. 8(d) and 9(d). For H_y, a holmium ion is mainly affected by oxygen ions numbered as 11 and 21 in Fig. 9(d), which can lead to the shift of a holmium ion in the $-x$ direction and an increase in the twist angle of the oxygen prism. The shift of a Ho^{3+} ion results in the appearance of electric dipole moment d_x directed opposite to the case of H_x, which explains the difference in the signs of polarization of the longitudinal and transverse ME_H-effects.[23]

Similar to the case of H_x, the magnetic susceptibility for H_y is most sensitive to distortions of the crystal lattice in the intermediate state b (Fig. 9(b)); therefore, the maximum in the field dependences $\Delta M(H)$ appears (Figs. (3a), (3b), (4a), and (4b)).

As we mentioned, the dependence $\Delta M(H)$ is odd for both measurement configurations E_x and E_y, i.e., the phase of the signal from coil 3 (Fig. 1) changes by 180° when the magnetic field direction reverses. In both cases, at H_y and H_{-y} the lattice strain leads to the change in the angle between the magnetic moment of a Ho^{3+} ion and the direction of field H. As a result, the magnetization of the crystal changes by the same law for both field directions, but the magnetization variation due to the ME_E-effect has the opposite sign because of the different magnetic moment direction. Hence, the voltage induced in the pick-up coil has different signs for the same phase of an AC voltage applied to the crystal at different directions of an external magnetic field.

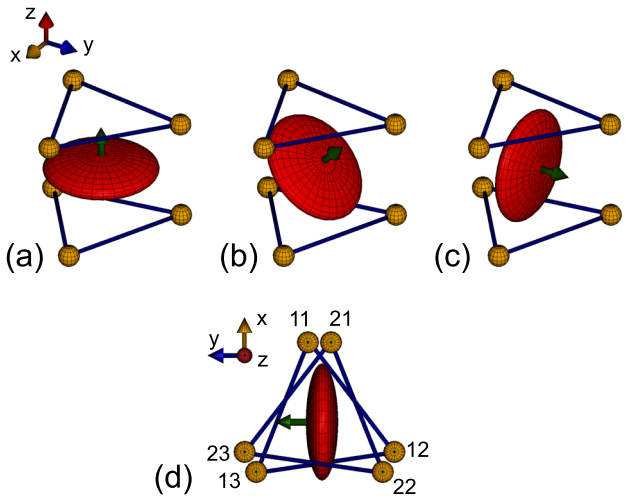

FIG. 9. Phases of rotation of Ho^{3+} ion at crystal magnetization (H||y).

As was demonstrated above, permittivity ε also depends on external magnetic field H (Figs. 7(a) and 7(b)). In the framework of the proposed model, we can explain the difference in the behaviors of $\varepsilon_x(H_y)$ and $\varepsilon_y(H_y)$. In applied external field H_y, the 4f subshell of a Ho^{3+} ion rotates to the state shown in Fig. 9(d). Applied electric field E_y causes the shift of a Ho^{3+} ion along the y axis relative to the oxygen surrounding. In strong magnetic fields, for electric field E_y, the shift of holmium ions along the y axis is prevented by oxygen ions 13, 23, 12, and 22 (Fig. 9(d)), whereas in the demagnetized state (Fig. 9(a)) the effect of the oxygen surrounding on a holmium ion is much weaker, so ε_y decreases with increasing field H_y.

It can be seen in Fig. 9(d) that the oxygen surrounding weakly resists the shift of a Ho^{3+} ion along the x axis, since the 4f subshell is located in the window formed by oxygen ions 13, 23, 12, and 22. Therefore, ε_x grows with field H_y.

CONCLUSIONS

For the first time, the ME_E-effect and permittivity of the $HoAl_3(BO_3)_4$ crystal were measured as functions of magnetic field and temperature. The ME_H-effect was additionally measured in the direction in which it was not observed before. The thermodynamic potential was considered for describing the magnetoelectric effect at low magnetic fields. It was suggested the magnetostriction described by Liang *et al.*[23] or magnetoelastic effect are responsible for the investigated phenomena. A qualitative microscopic model was proposed to explain the experimental data, as well as the results reported by Liang *et al.*[23] This mode is based on the interplay of configuration of 4f- electron subshell of the rare-earth element and applied magnetic or electric field. It was found the magnetoelectric effect can exist in crystals without the magnetic order or spontaneous polarization.

Clarification of the non-monotonic character of the dependences $\varepsilon(H)$ at high temperatures and $\varepsilon(T)$ in strong magnetic fields needs further investigations and is planned for very near future.

ACKNOWLEDGMENTS

This work was supported by Russian Foundation for Basic Research (Project Nos. 13-02-12442ofi_m2 and 14-02-00307). The authors are grateful to V. N. Ilyushchenko for the help in preparing of this manuscript.

[1]F. Hong, Z. Cheng, and X. Wang, J. Appl. Phys. **112**, 013920 (2012).
[2]J. Hwang, E. S. Choi, H. D. Zhou, J. Lu, and P. Schlottmann, Phys. Rev. B **85**, 024415 (2012).
[3]T. Kimura, T. Goto, H. Shintani, K. Ishizaka, T. Arima, and Y. Tokura, Nature (London) **426**, 55 (2003).

[4]J. Magesh, P. Murugavel, R. V. K. Mangalam *et al.*, J. Appl. Phys. **112**, 104116 (2012).
[5]X. K. Wei, T. Zou, F. Wang *et al.*, J. Appl. Phys. **111**, 073904 (2012).
[6]M. Shang, C. Zhang, T. Zhang *et al.*, Appl. Phys. Lett. **102**, 062903 (2013).
[7]R. Ramesh and N. A. Spaldin, Nature Mater. **6**, 21 (2007).
[8]Y. Kitagawa, Y. Hiraoka, T. Honda, T. Ishikura, H. Nakamura, and T. Kimura, Nature Mater. **9**, 797 (2010).
[9]W. Eerenstein, N. D. Mathur, and J. F. Scott, Nature **442**, 759 (2006).
[10]N. A. Hill *et al.*, J. Magn. Magn. Mater. **242**, 976 (2002).
[11]N. Hur *et al.*, Nature (London) **429**, 392 (2004).
[12]G. Lawes *et al.*, Phys. Rev. Lett. **95**, 087205 (2005).
[13]G. T. Rado and V. J. Folen, Phys. Rev. Lett. **7**, 310 (1961).
[14]M. Fiebig, J. Phys. D **38**, R123 (2005).
[15]J. E. Hamann-Borrero, S. Partzsch, S. Valencia *et al.*, Phys. Rev. Lett. **109**, 267202 (2012).
[16]R. P. Chaudhury, F. Yen, B. Lorenz *et al.*, Phys. Rev. B **80**, 104424 (2009).
[17]H. Schmid, in *Introduction to complex mediums for optics and electromagnetics*, edited by W. S. Wiegelhofer and A. Lakhtakia (SPIE Press, Bellingham, Washington, 2003), p. 176.
[18]J.-P. Rivera, Ferroelectrics **161**, 165 (1994).
[19]J.-P. Rivera, Ferroelectrics **161**, 147 (1994).
[20]D. N. Astrov, Zh. Exp. Teor. Fiz. **38**, 984 (1960) [Sov. Phys. JETP **11**, 708 (1960)].
[21]J.-C. Joubert *et al.*, J. Appl. Crystallogr. **1**, 318 (1968).
[22]J. A. Campa, C. Cascales, E. Gutierrez-Puebla *et al.*, Chem. Mater. **9**, 237 (1997).
[23]K.-C. Liang, R. P. Chaudhury, B. Lorenz *et al.*, Phys. Rev. B **83**, 180417(R) (2011).
[24]A. I. Begunov, A. A. Demidov, I. A. Gudim, and E. V. Eremin, JETP Lett. **97**, 528 (2013).
[25]D. Neogy, J. Magn. Magn. Mater. **154**, 127 (1996).
[26]R. P. Chaudhury, B. Lorenz, Y. Y. Sun *et al.*, Phys. Rev. B **81**, 220402 (R) (2010).
[27]V. I. Zinenko, M. S. Pavlovskiy, A. S. Krylov *et al.*, JETP **117**, 1032 (2013).
[28]A. D. Balaev and A. L. Freydman, Journal of Surface Investigation. X-ray, Synchrotron and Neutron Techniques **8**(1), 17–19 (2014).
[29]G. A. Smolenskii and I. E. Chupis, Usp. Fiz. Nauk. **137**, 415–448 (1982); Sov. Phys. Usp. **25**, 475–493 (1982).
[30]L. D. Landau and E. M. Lifshitz, *Electrodynamics of Continuous Media* (Pergamon Press, New York, 1984), pp.176 and 177.
[31]H. Shmid, in *Introduction to Complex Mediums for Optics and Electromagnetics*, edited by W. S. Weiglhofer and A. Lakhtakia. (SPIE Press, Washington, 2003), p. 169.
[32]M. E. Lines and A. M. Glass *Principles and Application of Ferroelectrics and Related Materials* (Claredon Press, Oxford, 1974), p. 608.
[33]M. Wietstruk, A. Melnikov, C. Stamm *et al.*, Phys. Rev. Lett. **106**, 127401 (2011).
[34]S A. Nikitin, "Magnetic Properties of Rare-Earth Metals and Their Alloys," (Moscow State University, Moscow, Russia, 1989).